Research Square

Preprints are preliminary reports that have not undergone peer review.
They should not be considered conclusive, used to inform clinical practice,
or referenced by the media as validated information.

Prediction and Optimization of Thermal Conductivity and Viscosity of Stable Plasmonic TiN Nanofluid Using Response Surface Method For Solar Thermal Application

Suhas Karmare
Government College of Engineering
Pradeep Patil
JSPM's Jayawantrao Sawant College of Engineering, Pune
Kishor Deshmukh (dkishor21@gmail.com)
KJ's Educational Institute , Trinity College of Engineering and Research

Research Article

Keywords: Nanofluid, TiN, RSM, Prediction, Optimization

Posted Date: September 15th, 2022

DOI: https://doi.org/10.21203/rs.3.rs-2057883/v1

License: This work is licensed under a Creative Commons Attribution 4.0 International License.
Read Full License

Prediction and Optimization of Thermal Conductivity and Viscosity of Stable Plasmonic TiN Nanofluid Using Response Surface Method For Solar Thermal Application

Kishor Deshmukh[1,2], Dr. Suhas Karmare[3], Dr. Pradeep Patil[4]

ABSTRACT

Nanofluids open a new dimension in solar thermal applications due to their enormous thermophysical properties. The preparation of stable, efficient, and low-cost nanofluids is an emerging area of research. According to NIMS (National Institute of Material Science) research, Titanium nitride (TiN) nanoparticles have localized surface plasmon resonance properties. It enables a superior photoabsorption feature. Titanium nitride (TiN) particles of 40-50 nm sizes were selected to prepare distilled water-based nanofluid at a 0-0.1% volume concentration range. The Thermal conductivity and viscosity of TiN nanofluids and base fluid are measured experimentally at temperatures 30℃ to 55℃. Determination of thermal conductivity and viscosity of nanofluid through experimentation is cumbersome. The present study deals with thermal conductivity and viscosity modeling of water-based stable plasmonic TiN nanofluid using the surface response method. ANOVA is used to determine the significance of input variables and their interaction. The performance of both predictive models was measured in terms of correlation coefficient (R^2) and mean square error (MSE) to acknowledge the best fit. The surface response method optimizes process parameters using reliable and efficient model results for maximum heat transfer enhancement. The maximum thermal conductivity (0.8848 W/mK) and minimum viscosity (0.7822 cP) obtained at 55℃ and 0.0535% volume concentration.

Keywords: *Nanofluid, TiN, RSM, Prediction, Optimization.*

List of symbol

TiN	Titanium nitride
LSPR	Localised Surface Plasmon Resonance
GA	Genetic Algorithm
K	Thermal Conductivity [W/mk]
NIMS	National Institute of Material Science
ANN	Artificial Neural Network
RSM	Surface Response Method
CFD	Computational Fluid Dynamics
SLS	Sodium Lauryl Sulfate
MSE	Mean Square Error
R^2	Correlation Coefficient
T	**Temperature [℃]**
I	**Electrical Current [mA]**
K	**Thermal Conductivity [W/mK]**
µ	**Viscosity [cP]**
R	**Elcrtical Resistance [Ohm]**
D	**Diameter [mm]**
A	**% Volume Concentration**
B	**Temperature [℃]**

Greek symbol

φ	Volume Concentration
µ	Dynamic Viscosity

[1] Research Scholar, KJ's Educational Institute Trinity College of Engineering and Research, Pune
[2]Assistant Professor, Amrutvahini College of Engineering, Sangamner
[3] Professor, Government College of Engineering, Avasari
[4]Professor, JSPM's Jayawantrao Sawant College of Engineering, Pune
[1]https://orcid.org/0000-0002-3131-9175

1. INTRODUCTION

According to the population division of the department of economic and social affairs, the world population is increasing dramatically by leap and bound. The industrial sector is expanding day by day to full fill the energy needs. Fossil fuel is the most common energy source. The continuous depletion and scarcity of fossil fuels motivate researchers to find renewable energy sources. Solar energy is the renewable energy source on earth. It has the potential to fulfill energy demands without polluting the environment [1][2][3]. Solar thermal collectors are used to harvest solar energy. Solar collectors absorb radiation and transfer absorbed energy to working fluid [1][2]. Conventional non-dielectric fluids like water, ethylene glycol, oils, and dielectric fluids like aliphatic liquids, silicone liquids, and fluorocarbon suffer from poor thermophysical properties. These properties limit the thermal performance of solar thermal collectors[1].

Choi (1995) (Argonne national Laboratory USA) developed a nanofluid by dispersing nanosize (<100nm) particles in the base fluid to enhance base fluid properties[4]. Hybrid nanofluids are the next version of nanofluids, prepared by suspending two or more types of nanoparticles in the base fluid[1]. Nanomaterials exhibit distinct thermal, physical, chemical, and mechanical properties due to more atomic atoms present on grain borders and a higher surface area-to-volume ratio. Nanofluid with tunable thermophysical properties will be a next-generation fluid. Sarkar et al.[5] summarized the scope and challenges for research in the fields of preparation, characterization, stability, cost, and applications of nanofluid[6]. Still, Nanofluid development and its application are in the infant stage. In recent decades research publications show significant improvement in thermophysical properties like thermal conductivity, convective heat transfer coefficient, density, viscosity, and thermal diffusivity of base fluid [7][6]. Nanofluid thermophysical properties depend upon the nature of the base fluid, particle type, temperature, volume concentration, size, and shape of nanoparticles. Thermal conductivity and viscosity of nanofluid have a substantial effect on heat transfer performance, hence considered the most vital properties[8]. In addition to heat transfer properties, the rheological behavior of nanofluids needs to be investigated simultaneously[9]. **Ishii et al.**[10] According to the MANA survey, water and air heating consume 55% of total energy. A research team proved experimentally that titanium nitride nanoparticles show plasmonic resonance properties[10]. Titanium nitride nanoparticles dispersed in water quickly. The TiN nanoparticles have a potential application area in solar heating and distillation of water. Titanium nitride nanoparticles are more efficient sunlight absorbers than gold and carbon nanoparticles due to the lossy resonances feature. Titanium nitride nanoparticles are more efficient sunlight absorbers than gold and carbon nanoparticles due to lossy resonance properties [10].

Continuous research work is going on to improve the performance of solar thermal collectors. The evacuated tube solar thermal collector performance depends upon inlet water temperature, flow rate, collector inclination, storage tank height, glass tube coating, and climate conditions such as heat flux, ambient temperature, wind speed, and relative humidity. To avoid the effect of fluctuating climatic conditions performance of the solar thermal collector was analyzed through indoor testing. Following gaps identified in previous research studies. **Deshmukh et al.** [11] did a comprehensive study on nanoparticles, nanofluids, and their applications. **Farid et al.** [12] studied solar-powered membrane distillation. The TiN nanoparticles deposited on a photothermal membrane by photo spray technique. Vapours are generated between the feed membrane interface and the TiN photothermal membrane. It is employed in saline feed stream water treatment and bulk water heating. The maximum effectiveness of the photothermal membrane was 66.7%. The TiN nanoparticles showed super natural photoabsorption capabilities. **Berkay et al.**[13] investigated titanium alloy thermal stress and strain. The highest values of Von Mises stress and shear stress observed at all temperatures. **Chan et al.** [14] examined the cocytoxity and antibacterial performance of TiN nanoparticles and laser nitrided titanium alloys. The antibacterial activities change the nanoparticle's size and shape. Nano-sized particles have larger surface areas, which results in greater interaction with bacterial cells. It affects the stability of the nanofluid. **Hussein et. al** [15] presented an in-depth analysis of nanotechnology applications in solar, hydrogen, wind, biomass, geothermal, and tidal energy. His studies suggest that nanomaterials can be employed to improve system efficiency and capture solar energy at a reasonable cost. **Rostami et al.**

[16] optimized the energy consumption of a flat plate solar thermal collector. An elliptical-shaped pipe and a water-based multiwall carbon nanotube nanofluid are used in the collector. For energy optimization, a semi-implicit finite volume approach is applied. The highest energy efficiency value was 7.1 %. **Ghodbane et. al** [17] investigated the performance of solar-powered ejector air conditioning systems under a given set of operational situations. This method is used a Fresnel solar reflector in the desert area. The thermal performance of the "STR" machine has reached 19.17%. **Hussein et al.** [18] explored a panoramic review of recent advances related to the application of nanotechnology in various types of solar collectors. Nanofluids can play a critical role in enhancing solar thermal collector efficiency. The nanofluid enhances the scattering and absorption of the incident radiation when passing through it. The use of nanofluid lowers convection and emissive heat loss in traditional collectors. **Amina et al.**[19] used corrugated inserts inside the absorber tube of a parabolic trough solar collector to improve overall heat transfer performance. The finite volume and the Monte Carlo raytracing method are used to examine flow and heat transfer characteristics. Heat transfer increases with an increase in corrugated insert twist ratio and a decrease in corrugation pitch. **Leong et al.** [20] evaluated current research on the application of nanofluids in solar collectors and the potential hurdles in developing an efficient nanofluid charge solar thermal collector. According to the literature findings, flat plate solar collectors are the most widely employed in nanofluid research. Commercialization of nanofluid charged thermal collectors is feasible if challenges such as stability, thermophysical property fluctuation, cost, and design optimization are appropriately addressed. **Sadhishkumar et. al** [21] summarize the previous works on solar water heating systems with various heat transfer enhancement techniques. It includes collector design, collector tilt angle, coating of pipes, fluid flow rate, thermal insulation, integrated collector storage, thermal energy storage, use of phase change materials, and insertion of twisted tapes. The survey depicts to date research focused on forced circulation mode only. There is scope for research in natural circulation solar water heating systems. Detail investigation of flow and thermal behavior is required to understand the complex dynamics behind the solar collector thermal performance enhancement. **Liu et al.** [22] used phase change material in the glazing unit. The influence of phase change material refractive index was on temperature rise, absorbance, transmittance, and reflectance of glazing units measured. For maximum solar energy collection, solid state phase change material with a high extinction coefficient is recommended. **Dong et al.** [23] evaluated the thermal performance of a PCM-filled double glazing unit. The purpose of the PCM material is to increase thermal storage capacity. PCM material has significant characteristics such as density, latent heat, thermal conductivity, specific heat, and melting point. **Sadik et al.** [24] compiled published articles on the use of nanofluid to improve forced convection heat transfer. According to the literature, nanofluids improve the thermophysical properties of conventional fluids by dispersing nanoparticles in these base liquids. Theoretical modelling of thermophysical characteristics is required to demonstrate the full potential of nanofluids for forced convection enhancement

Thermal conductivity and viscosity of nanofluid are a function of temperature, % volume concentration, and stability[25]. This dependency develops a complex relationship between thermophysical properties and variable parameters. The accurate prediction of thermophysical properties is not possible by conventional models. Soft computing techniques like RSM, ANN, NSGA, CFD, Particle swarm Technology, and fuzzy logic reduce experimentation cost and time[7]. An optimum volume concentration is required to design a sustainable and cost-effective system. The artificial neural network technique has an inbuilt prediction ability. **Seyed et al.**[26] proposed a combined artificial neural network (ANN) and genetic algorithm(GA) multiobjective optimization model. The ANN model determines the thermophysical properties of CuO/liquid paraffine nanofluid, and the GA model determines to minimize pressure drop and maximize the heat transfer coefficient. **Maqsood et al.** [27] did multiobjective optimization of thermal oil-based MWCNT nanofluid to maximize thermal conductivity and minimize viscosity. The RSM and ANN tools develop a predictive model. In addition to prediction, studied detailed optimization for four different cases according to applications. **Maqsood et al.** [28] investigated the thermophysical properties of nanofluid (fly ash+water) using the RSM tool. An empirical model was developed and tested with experimental data.

The aim was to determine optimum % volume concentration and thermophysical characteristics. **Barewar et al.** [29] synthesized Ag/ZnO-glycol hybrid nanofluid to investigate thermophysical properties experimentally. Experimental results compared with ANN model results. The correctness of the model is verified using the R^2, MSE, and average absolute relative deviation percent. **Amir et al.** [30] did geometrical parameters and flow characteristics optimization of water bases Al_2O_3 nanofluid inside a corrugated heat exchanger using a genetic algorithm. Al_2O_3 nanofluid acts as a cooling fluid. He considered corrugation length, depth, phase shift angle, nanoparticle concentration, and Reynolds number for optimization. MATLAB computational code used for modeling. **Arani et al.** [31] predicted the thermal conductivity of ferromagnetic nanofluid using ANN. He used a two-layer perceptron feedforward and backpropagation (BP-LM) training algorithm. The volume fraction, temperature, thermal conductivity of nanofluid, and base fluid consider the most promising input variables. He concluded ANN model has the capability of predicting thermal conductivity. **Sajid et al.** [32] summarised experimental, numerical, and ANN research to offer a thorough analysis of the thermal conductivity of hybrid nanofluids [32]. The impact of nanoparticle type, size, concentration, type of base fluid, temperature, surfactant addition, pH, and sonication time are examined for thermal conductivity prediction. Different machine learning methods for predicting thermophysical characteristics were discussed by Akbar et al. [33] ANN is considered as one of alluring method for simulating thermophysical characteristics is ANN [33]. The ANN model's performance was enhanced by using the proper optimization techniques to determine its ideal architecture design and reduce error margins[33].

In the last two decades, experimental and numerical studies have tried to bridge the gap between the selection of nanoparticles, base fluids, surfactants, nanofluid preparation, characterization, thermophysical properties investigation, prediction, optimization, and nanofluid application. The numerous grey areas discovered could be pivotal for the research community

- TiN nanoparticles have extraordinary lossy photoabsorption properties. Preparation, characterization, thermophysical properties investigation, and prediction with optimization are the best options to explore TiN nanofluid as a commercial thermic nanofluid for solar thermal applications [34].
- The effect of temperature and volume concentration on thermophysical properties is investigated independently, but their interaction has received little attention in the literature. The interaction effects are critical for determining the best nanofluid parameters for increased heat transfer coefficient. These effects could reduce the number of trials needed to achieve the desired heat transfer coefficient.
- There have been many studies on artificial intelligence techniques for modelling carbide, oxide, and caron allotropes-based nanofluid thermophysical properties, but very few on optimization.
- Among the available optimization techniques, the literature review recommends the Response Surface Methodology as a simple statistical method for multiobjective optimization. It demonstrates the effect of most and least dominant factors on response.

To the author's best knowledge, the study on the mentioned aspect has not been published yet. The current study investigates the thermal conductivity and viscosity of a water-based TiN nanofluid along with the individual and interactive effects of temperature (30–55°C) and volume concentration (0–0.1 %) on nanofluid properties. The attempt is to develop a confident and reliable approach that will allow the prediction of the thermal conductivity and viscosity of TiN nanofluid without physical experimentation due to high experimentation costs and time consumption. The Response Surface Model will predict thermophysical properties and solve the multiobjective optimization problem. RSM Full factorial design finds interactive effects and optimum conditions for maximum thermal conductivity and minimum viscosity. The TiN nanofluid optimum thermophysical properties can be used to design and develop low-cost, efficient, portable nanofluid-charged solar thermal collectors.

2. TIN NANOFLUID PREPARATION, CHARACTERIZATION, AND EXPERIMENTAL INVESTIGATION OF THERMOPHYSICAL PROPERTIES

2.1 Selection of Process Parameters

The literature depicts nanofluid thermal conductivity and viscosity play a crucial role in the micro convection phenomenon, hence considered a vital aspect while studying nanofluid. The thermal conductivity and viscosity of nanofluid increase with the increase in % the volume concentration of nanoparticles [7]. The increase in thermal conductivity causes heat transfer enhancement. An increase in viscosity increases pressure drop and decreases heat transfer rate [7]. The nanoparticles less than 100 nm give better stability and heat transfer performance. For this research average of 50 nm size nanoparticles were used. The nanoparticles start to agglomerate beyond 0.1 % volume concentration. So five concentration levels were chosen (0%, 0.025%, 0.050%, 0.075% 0.1%) for our investigation. The temperature of nanofluid inside solar thermal collector varied from 30°C to 60°C from 9.00 am to 5.0 pm. hence five temperature levels (35°C, 40°C, 45°C, 50°C, 55°C) are considered. Minitab 18 was used to perform DOE with the Taguchi method (two factors and a five-level design). Thermal conductivity and viscosity of TiN nanofluid measured experimentally using L25 orthogonal array.

2.2 Selection, Characterization of Nanomaterial, Base Fluid, Surfactant

The research team of NIMS & MANA (International Center for Materials Nanoarchitectonics) discovered that TiN nanofluid has superb sunlight absorption capability because of its LSPR property. Because of this unique feature, TiN nanoparticles are considered for this research work. Commercially available TiN nanoparticles (40-50 nm)[35] purchased from Intelligent Materials Pvt. Ltd, Punjab (India). Its mass fraction purity exceeds 99.9%. The water was distilled and subsequently treated by a Milli-Q water purification system (PureLab Flex 3, ELGA UK), and used as the base fluid for experimentation. The surfactants enhance the stability of nanofluids [7]. A surfactant converts the hydrophilic surface of the nanoparticles to hydrophobic and vice versa. LOBA Chemie Pvt. Ltd. branded extra pure needle-shaped sodium lauryl sulfate used as a surfactant because the base fluid contains an O-H bond [36]. Tables 1 and 2 show the properties of nanoparticles, base fluid, and surfactants.

The morphological structure of TiN particles analyze by the FESEM technique. Figure 1 (a) and Figure 1 (b) are SEM images of TiN nanoparticles captured by FESEM (FEI Nova NanoSEM 450, SPPU, Pune). High-resolution images of nanoparticles capture at 10 and 500nm scales at 100,000 magnification. These images show TiN nanoparticles have agglomerated and need sonication. The average particle size matches the supplier's test reports.

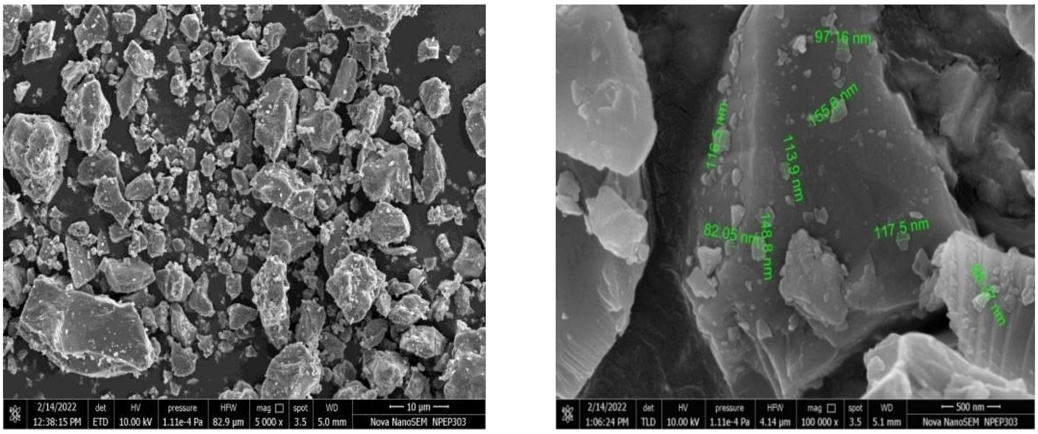

Figure 1 (a) Figure 1 (b)

Figure 1. FESEM of TiN Nanoparticle at 10μ and 500nm Scale

Table 1 Descriptions of Materials

Compound	CAS No	Source	Purity

TiN	25583-20-4	Intelligent Material Pvt. Ltd.	99.9%
SLS	151-21-3	LOBA Chemie Pvt. Ltd	99.0%
Distilled Water	NA	Milli- Q purification system	NA

Table 2 Chemical and Physical Properties of Material

Compound	Colour	Density (g/cm^3)	Form/ Shape	Melting Point (°C)	Partical Size (nm)	Molecular Weight (g/mol)	Thermal Conductivity (W/m°C)
TiN	Brown	5.24	Powder	2930	40-50	61.87	19.2
SLS	White	0.37	Needle	207		288.38	
Water	Colourless	0.994	Liquid	273	NA	18.01	0.6

2.3 Nanofluid Preparation

Nanofluid preparation is a crucial stage in nanofluid research. To achieve effectiveness in terms of heat transfer two-step method is followed. TiN nanoparticles were dispersed into distilled water (1000ml) with the volume fractions of 0.025%, 0.050%, 0.075%, and 0.1%[35]. The law of the mixture formula gives the quantity of TiN nanopowder required for a particular concentration. Sodium Lauryl Sulfate is used as a surfactant at a concentration of 1/10th of nanoparticles to improve its stability.

Figure 2. Preparation of Stable TiN Nanofluid

Figure 2 shows the steps followed to prepare a stable nanofluid. A calculated amount of dry titanium nitride powder and sodium lauryl sulfate (SLS) was weighed using a precision balance (Shimadzu AUX220) and poured into the base fluid. The strong Vander Walls force of attraction between TiN nanoparticles agglomerates nanoparticles. The magnetic stirrer (Remi 1MLH) breaks the powerful Vander wall attraction forces between nanoparticles. The Magnetic stirrer operates at 1000 rpm for 60 min. All the samples sonicate for 60 min in a bath-type ultrasonic stirrer at room temperature. The Probe-type ultrasonicator was used at the last stage to obtain a homogenous and stable nanofluid.

2.4 Nanofluids characterization and Thermophysical Properties Investigation

a. Stability and Particle Size

Stability indicates the nanoparticle rate of aggregation in the base fluid. The prepared TiN nanofluid is visually stable after 15 days. The SZ-100 HORIBA instrument from Amrutvahini College of Pharmacy, Sangamner, was chosen to measure the zeta potential and particle size of TiN nanofluid. The zeta potential value is a function of time. TiN nanoparticles with strong negative zeta potential do not tend to aggregate. Table 3 shows the zeta potential and corresponding particle size.

Table 3 Zeta Potential and Particle Size for Different % Volume Concentrations

Sample No.	% Vol. Concentration	Zeta potential (mV) ± 0.1 mV	Particle Size (nm) ± 0.3 nm
A1	0	0	100.0nm

A2	0.025	-61.6	117.3nm
A3	0.050	-61.1	141.5nm
A4	0.075	-37.1	144.3nm
A5	0.100	-30.1	151.1nm

b. Thermal Conductivity

Thermal conductivity is the ability of the material to conduct heat. The thermal conductivity of the nanofluid depends on the evenly distributed nanoparticles inside the base fluid. The Brownian movement of nanoparticles at the nanoscale level is considered a key mechanism for the micro convection in a nanofluid. Dr. Sonawane and Prof. Kokate developed the transient hot wire apparatus at Sapat College of Engineering in Nashik. He claims that the setup produces accurate results by eliminating natural convection effects. The TiN nanofluid thermal conductivity measured on the same apparatus. Figure 3 shows a schematic diagram of the transient hot-wire apparatus.

Figure 3. Transient Hot Wire Apparatus

The experimental setup includes two measuring cylinders, each 50 mm in diameter and 100 mm, 150 mm in length. The cylinders are in series combination and connected with the data acquisition system, electrical hardware, power supply, and computer. One cylinder serves as a compensating cylinder to eliminate possible convection losses in Platinium wire. The 50.8µm diameter platinium wire solder in a measuring cylinder with the help of a nut and bolt. A current-carrying wire heats the fluid inside the measuring cell. The temperature change is directly proportional to the change in Platinium wire resistance at different instants. The effective thermal conductivity of the nanofluids is determined by plotting the slope of the temperature increase of platinum wire against a logarithmic time interval [7][37]. The linear portion slope is determined by linear regression till unsigned residuals got. The linear portion slope is determined by linear regression till unsigned residuals got. The same procedure is adopted for deionized water, air, and toluene to measure thermal conductivity at room temperature to calibrate the instrument. After calibration of the transient hot wire apparatus measured thermal conductivity of TiN nanofluid. Table 5 gives thermal conductivity corresponding to temperatures.

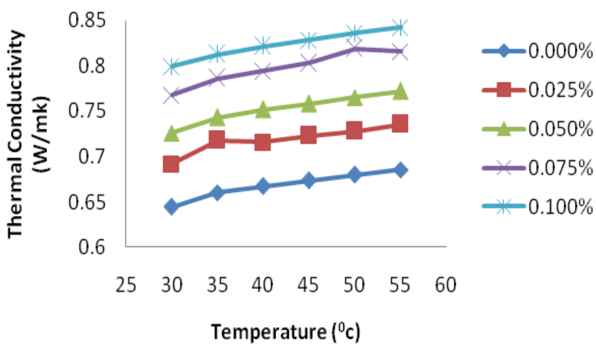

Figure 4. Thermal Conductivity Variation as A Function of % Volume Concentration

Figure 4 shows the variation of thermal conductivity against the temperature range for different volume concentrations. A maximum thermal conductivity of 0.8421% obtains at 0.1% volume concentration and 55°C. All nanofluid concentrations have the same trend as 0.1% volume concentration. The thermal conductivity enhancement was observed because of Brownian motion and the development of micro convection and conduction paths.

c. Viscosity

The viscosity is a fluid property that offers resistance to the movement of one layer to the adjacent layer. Fluid viscosity affects the friction between the contact surface and fluid molecules. The viscousness of nanofluid increases with % volume concentration. Nanofluid viscosity variation depends upon volume concentration, range of shear stress rate selected, base fluid type, agglomeration rate, temperature, purity, size, shape, type of nanoparticles, preparation, and dispersion method. The viscosity of TiN-Water nanofluid was measured using Brookfield Viscometer DV-I Prime (Figure 5) (SPPU, Chemistry department) at maximum % torque and 50rpm with accuracy ±0.1. Table 6 gives viscosity in cP corresponding to temperatures. The Brookfield viscometer calibrated using standard fluid supplied by Brookfield Engineering Laboratories. The liquid pour into the container. A constant temperature bath at 25°C maintains around the container. The spindle and speed are selected and set according to the standard procedure before taking the viscosity reading. Finally, viscosity was measured and compared with fluid viscosity limits.

Figure 5. Brookfield Viscometer

Figure 6 shows the viscosity variation against a temperature range for different volume concentrations. A minimum viscosity of 1.11 cP obtains at 0.1% volume concentration and 55°C. All nanofluid concentrations have the same trend as 0.1% volume concentration. A maximum enhancement of 19.05% obtained at 0.0.5% volume concentration. Volume concentration, cohesive forces, and adhesive forces between nanoparticles play an important role in this enhancement.

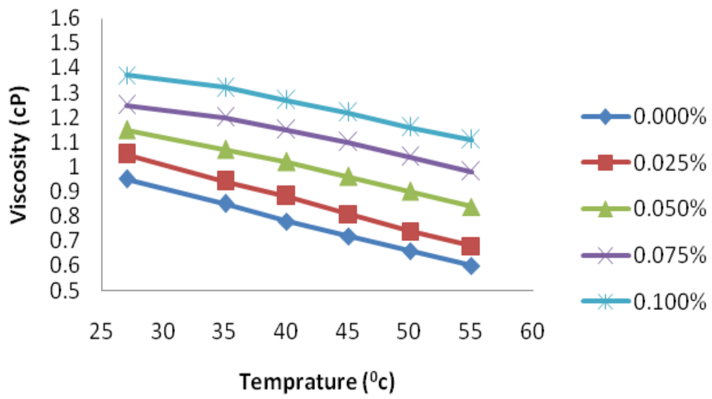

Figure 6. Viscosity Nanofluid vs. Temperature at a Different % Volume Concentration

3. Uncertainty Analysis

The purpose of uncertainty analysis is to quantify the output variability caused by input variability. Sundar et al. [38] described an uncertainty analysis procedure for estimating the associated errors caused by experimentation instruments. According to the uncertainty analysis, the maximum uncertainties are 0.46% in thermal conductivity and 1.052% in viscosity measurement. Table 4 depicts uncertainties involved during the investigation of thermophysical properties.

Table 4 Uncertainty of Instruments and TiN Nanofluid Thermophysical Properties

Sr. No	Name of Instrument	Variable Measured	Least Count of Instrument	Min. and Max. Value Measured	% Uncertainty
1	Transient Hot Wire Apparatus	Thermal Conductivity (K)	0.01W/mK	0.7170-0.7995 W/mk	0.460%
3	Brookfield Viscometer	Viscosity (μ)	0.01cP	0.95-1.2 cP	1.052%
4	Weighing Machine	Mass	0.0001 gm	1.3103-5.2552 gm	0.002%
5	Horiba SZ-1000	Stability	±0.1 mv	30.1-61.6 mv	0.162%
6	Horiba SZ-1000	Particle Size	0.3 nm	100-151.1 nm	0.198%

4. RSM-BASED PREDICTIVE MODEL

The surface response methodology is the most popular statistical and mathematical tool. It develops an empirical relationship between inputs and output variables considering the multiple regression techniques. The RSM concentrates on the effect of the least significant input variable on the response variable[28]. The main aim of the RSM is to develop thermal conductivity and viscosity predictive model. The volume concentration and temperature were considered input variables, and thermal conductivity and viscosity as the response variable. A second-order predictive model was developed by considering the mutual relationship between input and response variables.

$$Y = \beta_0 + \sum_{i=1}^{p} \beta_i X_i + \sum_{i=1}^{p} \beta_{ii} X_i^{\,2} + \sum_{i=1}^{p-1} \sum_{j=1}^{p} \beta_{ij} X_i X_j \qquad (1)$$

Where $\beta_0, \beta_{ii},$ and β_{ij} are the coefficient of the regression model. X_i and X_j are independent variables, and Y denotes the dependent response variable. In the last stage, ANOVA is used to investigate the importance of the predictive model and input variables. The ANOVA calculates the degree of freedom, the number of squared deviations, and the mean square error for each input. The input will consider as significant if the p-value is < 0.05.

$$K = 0.6132 + 1.817A + 0.00157B - 4.693A^2 - 0.000005B^2 + 0.00466\mathrm{AB} \qquad (2)$$

Eq. (2) gives the predictive model for thermal conductivity considering the interaction between input variables. Whereas K is thermal conductivity, A and B denote volume concentration temperature.

Table 5 shows an analysis of variance for the thermal conductivity model. The F value of the model is 732.58, and the p-value is 0.000. It shows the model is significance and acceptability of the developed model. The R^2 value is 99.48%. The thermal conductivity model shows volume concentration, temperature, and square of volume concentration are significant factors for thermal conductivity enhancement. Interaction between volume concentration and temperature does not contribute to enhancement.

Table 5 Analysis of Variance for Thermal Conductivity Model

Source	DF	Adj SS	Adj MS	F-Value	P-Value
Model	5	0.078738	0.015748	732.58	0.0000
Linear	2	0.078101	0.03905	1816.63	0.0000
% Volume Concentration (A)	1	0.075793	0.075793	3525.9	0.0000
Temperature (B)	1	0.002308	0.002308	107.36	0.0000
Square	2	0.000603	0.000302	14.03	0.0000
% Volume Concentration*% Volume Concentration (A^2)	1	0.000602	0.000602	28.01	0.0000
Temperature*Temperature (B^2)	1	0.000001	0.000001	0.05	0.825
2-Way Interaction	1	0.000034	0.000034	1.58	0.225
% Volume Concentration* Temperature (A*B)	1	0.000034	0.000034	1.58	0.225
Error	19	0.000408	0.000021		
Total	24	0.079146			

$$\mu = 1.410 + 3.41A - 0.0173B - 1.6A^2 - 0.000034B^2 + 0.0496AB \quad (3)$$

Eq. (3) gives the viscosity predictive model considering the interaction between input variables. Whereas μ is viscosity, A and B denote volume concentration and temperature. Table 6 show an analysis of variance for the viscosity model. The F value of the model is 127.77, and the p-value is 0.000. It shows the significance and acceptability of the developed model. The R^2 value is 97.11%. The viscosity model shows volume concentration and temperature are significant factors for viscosity enhancement. Individual and mutual interaction between volume concentration and the temperature does not contribute to enhancement.

Table 6 Analysis of Variance for Viscosity Model

Source	DF	Adj SS	Adj MS	F-Value	P-Value
Model	5	1.11529	0.223057	127.77	0.0000
Linear	2	1.11132	0.555661	318.3	0.0000
% Volume Concentration (A)	1	0.17287	0.172872	99.03	0.0000
Temperature (B)	1	0.93845	0.93845	537.57	0.0000
Square	2	0.00012	0.000061	0.03	0.966
% Volume Concentration*% Volume Concentration (A^2)	1	0.00005	0.000051	0.03	0.866
Temperature*Temperature (B^2)	1	0.00007	0.00007	0.04	0.843
2-Way Interaction	1	0.00384	0.003844	2.2	0.154
% Volume Concentration* Temperature (A*B)	1	0.00384	0.003844	2.2	0.154
Error	19	0.03317	0.001746		
Total	24	1.14846			

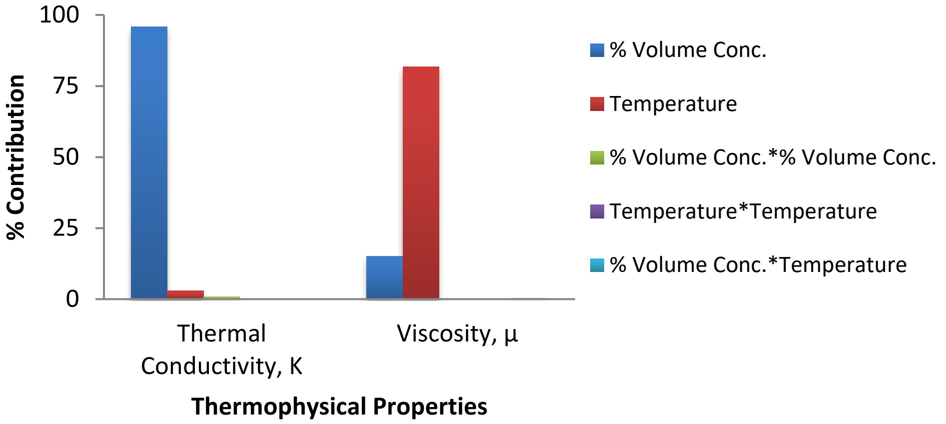

Figure 7. Contribution of Input Parameters for Thermal Conductivity and Viscosity Enhancement

Figure 7 shows the contribution of volume concentration, temperature, and mutual interaction. The most significant input variable is volume concentration (95.76%) followed by temperature (2.91%) for thermal conductivity enhancement, and temperature (81.71%) followed by volume concentration (15.05%) for viscosity enhancement. Figure 8 and Figure 9 show a scatter plot of experimental thermal conductivity and viscosity values with predicted values. The R^2 value of both models is between 97 and 98 %. Higher R^2 values show the reliability and efficiency of predicted models.

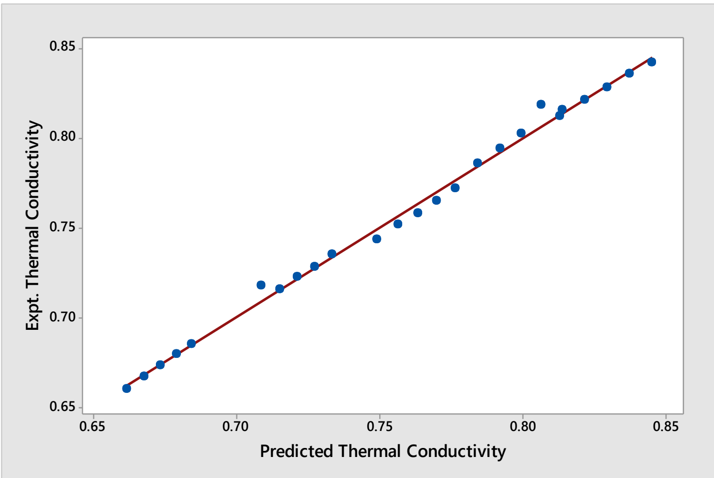

Figure 8. Scatterplot of Experimental Thermal Conductivity and Predicted Thermal Conductivity of TiN Nanofluid.

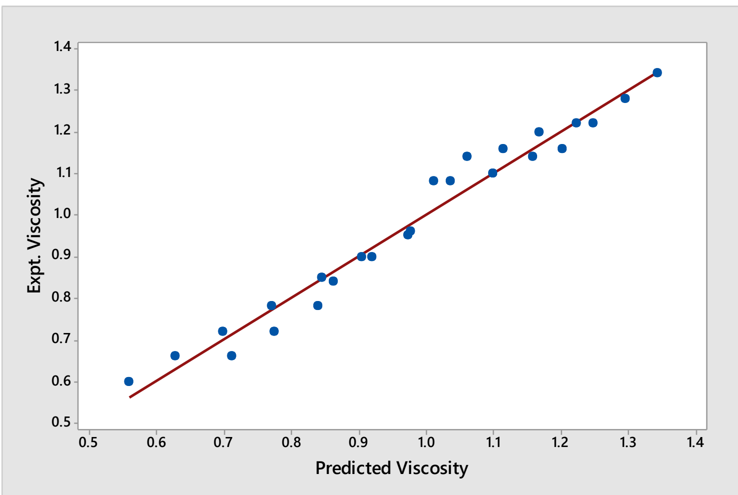

Figure 9. Scatterplot of Experimental Viscosity and RSM Predicted TiN Nanofluid Viscosity.

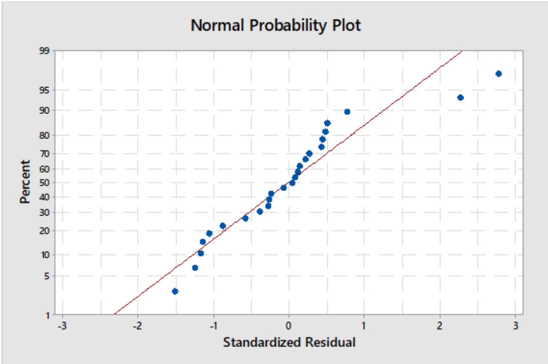

Figure 10. (a)

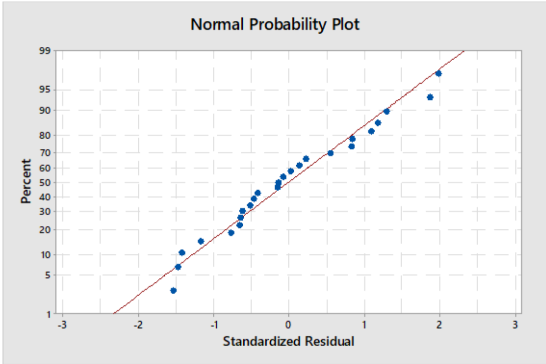

Figure 10 (b)

Figure 10. Normal Probability Plot of (a) Predicted Thermal Conductivity (b) Predicted Viscosity of TiN Nanofluid.

The adequacy test and outlier plot test examine accuracy after model development. Figure 10 (a) and Figure 10 (b) show residual plots for thermal conductivity and viscosity models. The results are randomly distributed near the regression line and do not follow any pattern. It confirms that it is suitable for optimization and prediction. After data prediction, outlier detection and removal is an important step. Outlier points never follow the trend of other data points. Figure 11 shows an outlier plot for thermal conductivity and viscosity. All the data points fall within the allowable range of the predictive model. Constant outlier plots assure that RSM predictive models are reliable and give correct predictions.

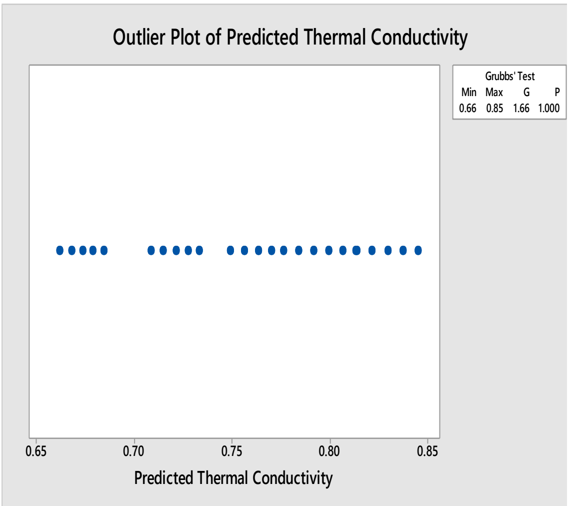

Figure 11. (a)

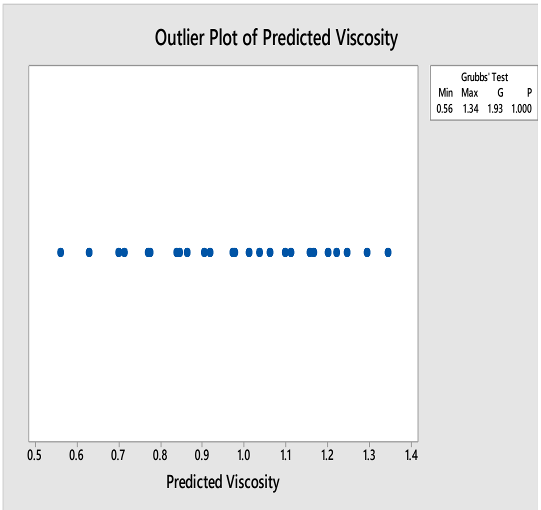

Figure 11. (a)

Figure 11. Outlier plot of (a) Predicted Thermal conductivity (b) Predicted Viscosity of TiN nanofluid.

The contour surface response plot provides the influence of each parameter on thermal conductivity enhancement. Figure 12 (a) shows thermal conductivity of TiN nanofluid increases with an increase in % volume concentration and temperature. Maximum thermal conductivity of 0.84 w/mk obtain at 0.1 % volume concentration and 55°C.

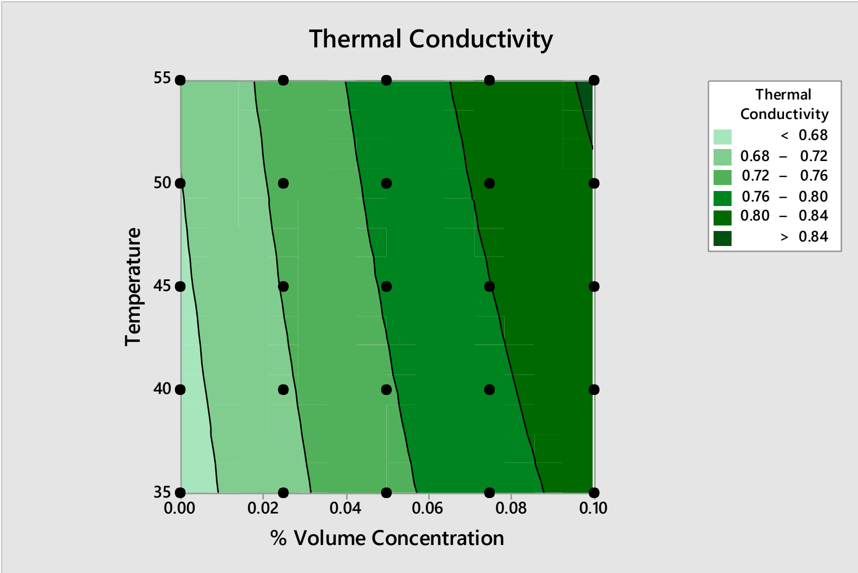

Figure 12 (a). 3D Contour Plots for Experimental and Corresponding RSM Predicted Thermal Conductivity.

Figure 12 (b) shows Viscosity of TiN nanofluid increases with an increase in % volume concentration and decreases with temperature. Minimum viscosity of 0.6 cP obtained at 0 % volume concentration and 55°C.

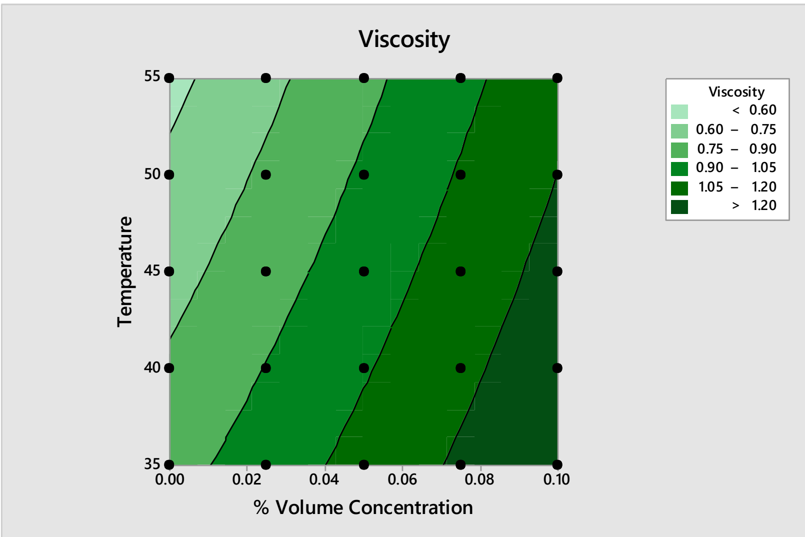

Figure 12 (b). 3D Contour Plots for Experimental and Corresponding RSM Predicted Viscosity.

5. COMPARATIVE ERROR ANALYSIS OF EXPERIMENTAL RESULTS RSM MODEL REULS

A comparative error analysis of the RSM model perform in terms of correlation coefficient (R2), root mean square (RMSE), standard error of prediction (SEP), and average absolute deviation (AAD). Maximum R^2 shows the closeness of data points to the regression line. The minimum MSE signifies how far the data points are from the regression line

$$R^2 = 1 - \frac{\sum_{i=1}^{n}(Y_{Pred} - Y_{Exp})^2}{\sum_{i=1}^{n}(Y_{Pred} - Y_{mean})^2} \quad (4)$$

$$RMSE = \sqrt{\frac{\sum_{i=1}^{n}(Y_{Pred} - Y_{Exp})^2}{n}} \quad (5)$$

$$\text{SEP}\ (\%) = \frac{\text{RMSE}}{Y_{mean}} \times 100 \quad (6)$$

$$\text{AAD}\ (\%) = \frac{100}{n} \times \sum_{i=1}^{n} \frac{(Y_{Pred} - Y_{Exp})^2}{Y_{Exp}} \quad (7)$$

Y_{pred} is predicted data, Y_{exp} is the experimental data, Y_{mean} is the mean of experimental data, and n is the number of experiments. Table 7 show experimental and predicted values of thermal conductivity and viscosity. The R^2 value of the RSM thermal conductivity model is 99.48%. It indicates RSM thermal conductivity model predicts closer accurate data. The R^2 value of the RSM viscosity model is 96.97 %. It reflects RSM thermal conductivity, and the viscosity model predicts closer accurate data.

Table 7 Experimental and RSM Predicted Thermal Conductivity and Viscosity of TiN Nanofluid

Sr. No	% Volume Concentration	Temperature °C	Experimental		Response Surface Method	
			K (W/mK)	μ (cP)	K (W/mK)	μ (cP)
1.	0	35	**0.6602**	**0.8500**	0.6621	0.8457
2.	0	40	**0.6671**	**0.7800**	0.6681	0.7719
3.	0	45	**0.6736**	**0.7200**	0.6739	0.6999
4.	0	50	**0.6797**	**0.6600**	0.6794	0.6295
5.	0	55	**0.6854**	**0.6000**	0.6847	0.5609
6.	0.025	35	**0.7178**	**0.9500**	0.7087	0.9733
7.	0.025	40	**0.7159**	**0.9000**	0.7153	0.9057
8.	0.025	45	**0.7228**	**0.7800**	0.7216	0.8399
9.	0.025	50	**0.7282**	**0.7200**	0.7277	0.7757
10.	0.025	55	**0.7353**	**0.6600**	0.7336	0.7133
11.	0.05	35	**0.7433**	**1.1000**	0.7494	1.0989
12.	0.05	40	**0.7516**	**1.0800**	0.7566	1.0375
13.	0.05	45	**0.7582**	**0.9600**	0.7635	0.9779
14.	0.05	50	**0.7651**	**0.9000**	0.7702	0.9199
15.	0.05	55	**0.7723**	**0.8400**	0.7766	0.8637
16.	0.075	35	**0.7860**	**1.2200**	0.7843	1.2225
17.	0.075	40	**0.7941**	**1.2000**	0.7920	1.1673
18.	0.075	45	**0.8028**	**1.1600**	0.7995	1.1139
19.	0.075	50	**0.8188**	**1.1400**	0.8068	1.0621
20.	0.075	55	**0.8158**	**1.0800**	0.8138	1.0121
21.	0.1	35	**0.8124**	**1.3400**	0.8132	1.3441
22.	0.1	40	**0.8217**	**1.2800**	0.8216	1.2951
23.	0.1	45	**0.8285**	**1.2200**	0.8296	1.2479
24.	0.1	50	**0.8359**	**1.1600**	0.8375	1.2023
25.	0.1	55	**0.8421**	**1.1400**	0.8451	1.1585
				R^2	99.48%	96.97%
				MSE	1.634E-05	8.82E-05

6. MODEL VALIDATION

The predicted models are validated at 0.04 % volume concentration at 42°C to check the conformity of the predicted models. Table 8 shows the validation and conformity of predicted models with a maximum error of ±2.00 %. The RSM thermal conductivity and viscosity models are valid for % concentration (0-0.1%) and temperatures (0-55°C). The RSM thermal conductivity and viscosity model predict reliable and efficient results.

Table 8 Predicted Model Validation

Sr. No	% Volume Concentration	Temperature °C	RSM		Experimental 1		Experimental 2		Experimental 3	
			K W/mK	µ cP	K W/mK	µ cP	K W/mK	µ cP	K W/mK	µ cP
1	0.04	42	0.7433	0.8405	0.733	0.841	0.724	0.839	0.742	0.840
% Error					-1.38	0.049	-2.669	-0.189	-0.178	-0.070

7. OPTIMIZATION

The optimization method finds the best solution within available boundary conditions. The challenge for nanofluid commercialization is fluctuating thermophysical properties. The stable nanofluid thermophysical properties depend upon % volume concentration and temperature. Thermal conductivity of nanofluid increases with an increase in % volume concentration and temperature and encourage heat transfer enhancement. The viscosity of nanofluid increases with an increase in % volume concentration decreases with temperature and limits heat transfer enhancement.

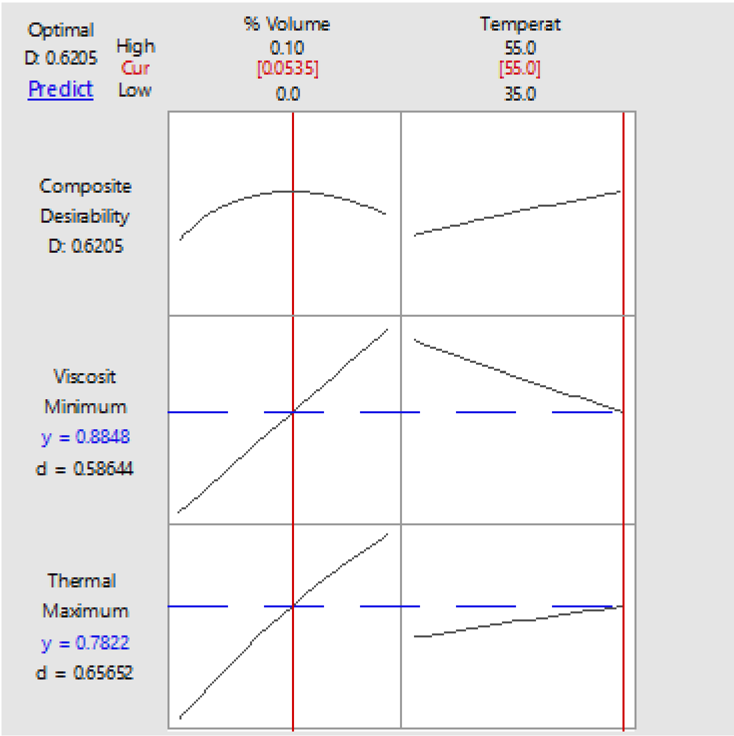

Figure 13. Optimization of TiN Nanofluid Thermal Conductivity and Viscosity

The Titanium nitride (TiN) nanofluid is suitable for solar thermal applications due to its LSPR property. Figure 13 shows optimization of TiN nanofluid. Solar thermal applications require nanofluid having maximum thermal conductivity and minimum viscosity at operating temperature. The RSM tool predicts accurate data same dataset used for optimization. Maximum thermal conductivity of 0.8848 w/mk and minimum viscosity 0.7822 cP achieved at 55°C with 0.0535% volume concentration.

CONCLUSION

In this study, preparation, characterization, and experimental investigation of TiN nanofluid thermophysical properties carry out to reach maximum thermal conductivity and minimum viscosity requirements for solar thermal applications. This paper focuses on the prediction and optimization of thermal conductivity and viscosity. The TiN nanofluid shows long-duration stability with enhanced thermophysical properties. Determination of thermophysical properties is a time-consuming and costly process. Hence, RSM-based thermal conductivity and viscosity predictive models are developed as functions of volume concentration, temperature, and interaction between them. The ANOVA results show that the volume concentration and temperature interaction have no significant effect on enhancement. The RSM-based thermal conductivity and viscosity model gives confident, reliable, and precise results.

$$K = 0.6132 + 1.817A + 0.00157B - 4.693A^2 - 0.000005B^2 + 0.00466\text{AB}$$

$$\mu = 1.410 + 3.41A - 0.0173B - 1.6A^2 - 0.000034B^2 + 0.0496\text{AB}$$

The RSM optimization approach finds maximum thermal conductivity and minimum viscosity. The objective functions are developed by considering thermal conductivity and viscosity experimental data. The optimum volume concentration and temperature are 0.0535% and 55°C for maximum thermal conductivity (0.8848 w/mk) and minimum viscosity (0.7822 cP). The predicted and optimized results are valid for 0-0.1% volume concentration and a 35-55°C temperature. The optimum operating conditions will reduce cost and system size. The conformity test performed on the thermal conductivity and viscosity models. The conformity test result shows ± 1.5% deviation. Stable TIN nanofluid worthiness is found in terms of photoabsorption and thermophysical properties for solar applications. There is scope for research to predict more than one thermophysical property using different intelligent techniques.

ACKNOWLEDGMENT

The authors would like to acknowledge the Amrutvahini Pharmacy College, Sangamner, for providing a nanofluid preparation and testing facility and special thanks to Prof. Kokate, Gokhale Education Society's R.H.Sapat College of Engineering, Management Studies and Research and Dr. Kodam Department of Chemistry SPPU, Pune for availing thermal conductivity and viscosity test facility.

DECLARATION OF INTERESTS

- The authors declare that they have no known competing financial interests or personal relationships that could have appeared to influence the work reported in this paper.
- The authors declare the following financial interests/personal relationships which may be considered as potential competing interests:

Deshmukh Kishor Bhausaheb reports equipment, drugs, or supplies was provided by Amrutvahini College of Pharmacy. Deshmukh Kishor Bhausaheb reports equipment, drugs, or supplies was provided by R H Sapat College of Engineering Management Studies and Research. Deshmukh Kishor Bhausaheb reports equipment, drugs, or supplies was provided by Department of Chemistry, SPPU, Pune. Deshmukh Kishor Bhausaheb reports statistical analysis was provided by Amrutvahini College of Engineering.

BIBLIOGRAPHY

[1] M. A. Sabiha, R. Saidur, S. Hassani, Z. Said, and S. Mekhilef, "Energy performance of an evacuated tube solar collector using single walled carbon nanotubes nanofluids," *Energy Convers. Manag.*, vol. 105, pp. 1377–1388, 2015, doi: 10.1016/j.enconman.2015.09.009.

[2] I. M. Mahbubul, M. M. A. Khan, N. I. Ibrahim, H. M. Ali, F. A. Al-Sulaiman, and R. Saidur,

"Carbon nanotube nanofluid in enhancing the efficiency of evacuated tube solar collector," *Renew. Energy*, vol. 121, pp. 36–44, 2018, doi: 10.1016/j.renene.2018.01.006.
[3] S. Iranmanesh, M. Mehrali, E. Sadeghinezhad, B. C. Ang, H. C. Ong, and A. Esmaeilzadeh, "Evaluation of viscosity and thermal conductivity of graphene nanoplatelets nanofluids through a combined experimental–statistical approach using respond surface methodology method," *Int. Commun. Heat Mass Transf.*, vol. 79, pp. 74–80, 2016, doi: 10.1016/j.icheatmasstransfer.2016.10.004.
[4] A. R. I. Ali and B. Salam, "A review on nanofluid: preparation, stability, thermophysical properties, heat transfer characteristics and application," *SN Appl. Sci.*, vol. 2, no. 10, 2020, doi: 10.1007/s42452-020-03427-1.
[5] J. Sarkar, P. Ghosh, and A. Adil, "A review on hybrid nanofluids: Recent research, development and applications," *Renew. Sustain. Energy Rev.*, vol. 43, pp. 164–177, 2015, doi: 10.1016/j.rser.2014.11.023.
[6] K. S. Deshmukh K, "A Review on Augmentation of Convective Heat Transfer Techniques in Solar Water Heating," *J. Therm. Energy Syst.*, vol. 4, no. 3, pp. 29–40, 2019, doi: http://doi.org/10.5281/zenodo.3542729.
[7] N. K. Cakmak, Z. Said, L. S. Sundar, Z. M. Ali, and A. K. Tiwari, "Preparation, characterization, stability, and thermal conductivity of rGO-Fe3O4-TiO2 hybrid nanofluid: An experimental study," *Powder Technol.*, vol. 372, pp. 235–245, 2020, doi: 10.1016/j.powtec.2020.06.012.
[8] Y. Cao, A. Khan, A. Abdi, and M. Ghadiri, "Combination of RSM and NSGA-II algorithm for optimization and prediction of thermal conductivity and viscosity of bioglycol/water mixture containing SiO2 nanoparticles," *Arab. J. Chem.*, vol. 14, no. 7, p. 103204, 2021, doi: 10.1016/j.arabjc.2021.103204.
[9] D. Yadav, P. Dansena, S. K. Ghosh, and P. K. Singh, "A unique multilayer perceptron model (ANN) for different oxide/EG nanofluid's viscosity from the experimental study," *Phys. A Stat. Mech. its Appl.*, vol. 549, p. 124030, 2020, doi: 10.1016/j.physa.2019.124030.
[10] S. Ishii, R. P. Sugavaneshwar, and T. Nagao, "Titanium Nitride Nanoparticles as Plasmonic Solar-Heat Transducers," *J. Phys. Chem.*, 2015, doi: 10.1021/acs.jpcc.5b09604.
[11] K. B. DESHMUKH and S V KARMARE, "A review on convective heat augmentation techniques in solar thermal collector using nanofluid," *J. Therm. Eng.*, vol. 7, no. 5, pp. 1257–1266, 2021, doi: 10.18186/thermal.978064.
[12] M. U. Farid, J. A. Kharraz, and A. K. An, "Plasmonic Titanium Nitride Nano-enabled Membranes with High Structural Stability for Efficient Photothermal Desalination," *ACS Appl. Mater. Interfaces*, vol. 13, no. 3, pp. 3805–3815, 2021, doi: 10.1021/acsami.0c17154.
[13] B. Berkay ERGENE, "DETERMINATION OF THERMAL STRESS AND ELONGATION ON DIFFERENT CERAMIC COATED Ti-6Al-4V ALLOY AT ELEVATED TEMPERATURES BY FINITE ELEMENT METHOD," vol. 38, no. 4, pp. 2013–2026, 2020.
[14] C. W. Chan, J. Quinn, I. Hussain, L. Carson, G. C. Smith, and S. Lee, "A promising laser nitriding method for the design of next generation orthopaedic implants: Cytotoxicity and antibacterial performance of titanium nitride (TiN) wear nano-particles, and enhanced wear properties of laser-nitrided Ti6Al4V surfaces," *Surf. Coatings Technol.*, vol. 405, no. September 2020, p. 126714, 2021, doi: 10.1016/j.surfcoat.2020.126714.
[15] A. K. Hussein, "Applications of nanotechnology in renewable energies - A comprehensive overview and understanding," *Renew. Sustain. Energy Rev.*, vol. 42, pp. 460–476, 2015, doi: 10.1016/j.rser.2014.10.027.
[16] S. Rostami, M. Sepehrirad, A. Dezfulizadeh, A. K. Hussein, A. S. Goldanlou, and M. S. Shadloo, "Exergy optimization of a solar collector in flat plate shape equipped with elliptical pipes filled with turbulent nanofluid flow: A study for thermal management," *Water (Switzerland)*, vol. 12, no. 8, 2020, doi: 10.3390/w12082294.
[17] M. Ghodbane, B. Boumeddane, and A. K. Hussein, "Performance Analysis of A Solar-Driven Ejector Air Conditioning System Under EL-Oued Climatic Conditions, Algeria," *J. Therm. Eng.*, vol. 7, no. 1, pp. 172–189, 2021, doi: 10.18186/thermal.847334.
[18] A. K. Hussein, "Applications of nanotechnology to improve the performance of solar collectors - Recent advances and overview," *Renew. Sustain. Energy Rev.*, vol. 62, no. 1, pp. 767–792, 2016, doi: 10.1016/j.rser.2016.04.050.
[19] A. Benabderrahmane, A. Benazza, and A. K. Hussein, "Heat Transfer Enhancement Analysis of Tube Receiver for Parabolic Trough Solar Collector with Central Corrugated Insert," *J. Heat Transfer*, vol. 142, no. 6, pp. 1–8, 2020, doi: 10.1115/1.4046440.
[20] K. Y. Leong, H. C. Ong, N. H. Amer, M. J. Norazrina, M. S. Risby, and K. Z. Ku Ahmad, "An

overview on current application of nanofluids in solar thermal collector and its challenges," *Renew. Sustain. Energy Rev.*, vol. 53, pp. 1092–1105, 2016, doi: 10.1016/j.rser.2015.09.060.

[21] S. Sadhishkumar and T. Balusamy, "Performance improvement in solar water heating systems - A review," *Renew. Sustain. Energy Rev.*, vol. 37, pp. 191–198, 2014, doi: 10.1016/j.rser.2014.04.072.

[22] C. Liu, Y. Wu, D. Li, T. Ma, A. K. Hussein, and Y. Zhou, "Investigation of thermal and optical performance of a phase change material–filled double-glazing unit," *J. Build. Phys.*, vol. 42, no. 2, pp. 99–119, 2018, doi: 10.1177/1744259117708734.

[23] D. Li, Z. Li, Y. Zheng, C. Liu, A. K. Hussein, and X. Liu, "Thermal performance of a PCM-filled double-glazing unit with different thermophysical parameters of PCM," *Sol. Energy*, vol. 133, pp. 207–220, 2016, doi: 10.1016/j.solener.2016.03.039.

[24] S. Kakac and A. Pramuanjaroenkij, "Review of convective heat transfer enhancement with nanofluids," *Int. J. Heat Mass Transf.*, vol. 52, no. 13–14, pp. 3187–3196, 2009, doi: 10.1016/j.ijheatmasstransfer.2009.02.006.

[25] S. S. Sonawane and V. Juwar, "Optimization of conditions for an enhancement of thermal conductivity and minimization of viscosity of ethylene glycol based Fe3O4 nanofluid," *Appl. Therm. Eng.*, vol. 109, no. November, pp. 121–129, 2016, doi: 10.1016/j.applthermaleng.2016.08.066.

[26] S. A. Bagherzadeh, M. T. Sulgani, V. Nikkhah, M. Bahrami, A. Karimipour, and Y. Jiang, "Minimize pressure drop and maximize heat transfer coefficient by the new proposed multi-objective optimization/statistical model composed of 'ANN + Genetic Algorithm' based on empirical data of CuO/paraffin nanofluid in a pipe," *Phys. A Stat. Mech. its Appl.*, vol. 527, p. 121056, 2019, doi: 10.1016/j.physa.2019.121056.

[27] K. Maqsood *et al.*, "Multi-objective optimization of thermophysical properties of multiwalled carbon nanotubes based nanofluids," *Chemosphere*, vol. 286, p. 131690, Jan. 2022, doi: 10.1016/J.CHEMOSPHERE.2021.131690.

[28] K. Maqsood, "Multiobjective optimization of thermophysical properties of indonesian fly-ash nanofluid," *Mater. Today Proc.*, vol. 49, no. xxxx, pp. 1255–1262, 2022, doi: 10.1016/j.matpr.2021.06.304.

[29] S. D. Barewar, S. Tawri, and S. S. Chougule, "Experimental investigation of thermal conductivity and its ANN modeling for glycol-based Ag/ZnO hybrid nanofluids with low concentration," *J. Therm. Anal. Calorim.*, vol. 6, no. 3, pp. 1779–1790, 2019, doi: 10.1007/s10973-019-08618-6.

[30] A. Ebrahimi-Moghadam and A. J. Moghadam, "Optimal design of geometrical parameters and flow characteristics for Al2O3/water nanofluid inside corrugated heat exchangers by using entropy generation minimization and genetic algorithm methods," *Appl. Therm. Eng.*, pp. 889–898, 2019, doi: 10.1016/j.applthermaleng.2018.12.068.

[31] J. B. Arani, A. Narooei, C. T. Branch, S. Faculty, and A. Branch, "Nanofluid Thermal Conductivity Prediction Model Based on Artificial Neural Network," *Trans. Phenom. Nano Micro Scales*, vol. 4, no. 2, pp. 41–46, 2016, doi: 10.7508/tpnms.2016.02.005.

[32] M. U. Sajid and H. M. Ali, "Thermal conductivity of hybrid nanofluids : A critical review," *Int. J. Heat Mass Transf.*, vol. 126, pp. 211–234, 2018, doi: 10.1016/j.ijheatmasstransfer.2018.05.021.

[33] A. Maleki, A. Haghighi, and I. Mahariq, "Machine learning-based approaches for modeling thermophysical properties of hybrid nanofluids: A comprehensive review," *J. Mol. Liq.*, vol. 322, p. 114843, 2021, doi: 10.1016/j.molliq.2020.114843.

[34] K. Deshmukh, S. Karmare, and D. Raut, "Preparation , characterization and experimental investigation of thermophysical properties of stable TiN nanofluid for solar thermal application National Institute of Material Science," *J. Brazilian Soc. Mech. Sci. Eng.*, vol. 2, 2022, doi: 10.1007/s40430-022-03733-2.

[35] S. Kumar, N. Chander, V. K. Gupta, and R. Kukreja, "Progress, challenges and future prospects of plasmonic nanofluid based direct absorption solar collectors – A state-of-the-art review," *Sol. Energy*, vol. 227, no. October 2020, pp. 365–425, 2021, doi: 10.1016/j.solener.2021.09.008.

[36] S. Sonawane, K. Patankar, A. Fogla, B. Puranik, U. Bhandarkar, and S. Sunil Kumar, "An experimental investigation of thermo-physical properties and heat transfer performance of Al2O3-Aviation Turbine Fuel nanofluids," *Appl. Therm. Eng.*, vol. 31, no. 14–15, pp. 2841–2849, 2011, doi: 10.1016/j.applthermaleng.2011.05.009.

[37] Y. Jannot, A. Degiovanni, V. Schick, and J. Meulemans, "Apparent thermal conductivity measurement of anisotropic insulating materials at high temperature by the parallel hot-wire

method," *Int. J. Therm. Sci.*, vol. 160, no. September 2020, p. 106672, 2021, doi: 10.1016/j.ijthermalsci.2020.106672.

[38] L. S. Sundar and K. V. Sharma, "Turbulent heat transfer and friction factor of Al 2 O 3 Nanofluid in circular tube with twisted tape inserts," *Int. J. Heat Mass Transf.*, vol. 53, no. 7–8, pp. 1409–1416, 2010, doi: 10.1016/j.ijheatmasstransfer.2009.12.016.